

Accepted Article

Title: Valeric Biofuel Production from γ -Valerolactone over Bifunctional Catalysts with Moderate Noble-Metal Loading

Authors: Karla G. Martínez Figueredo, Emanuel M. Virgilio, Darío J. Segobia, and Nicolás Maximiliano Bertero

This manuscript has been accepted after peer review and appears as an Accepted Article online prior to editing, proofing, and formal publication of the final Version of Record (VoR). This work is currently citable by using the Digital Object Identifier (DOI) given below. The VoR will be published online in Early View as soon as possible and may be different to this Accepted Article as a result of editing. Readers should obtain the VoR from the journal website shown below when it is published to ensure accuracy of information. The authors are responsible for the content of this Accepted Article.

To be cited as: *ChemPlusChem* 10.1002/cplu.202100249

Link to VoR: <https://doi.org/10.1002/cplu.202100249>

COMMUNICATION

Valeric Biofuel Production from γ -Valerolactone over Bifunctional Catalysts with Moderate Noble-Metal Loading

B.Sc. Karla G. Martínez Figueredo ^[a], B.Ch.E. Emanuel M. Virgilio ^[a], Dr. Darío J. Segobia ^[a] and Dr. Nicolás M. Bertero ^{*[a]}

[a] Grupo de Investigaciones en Ciencia e Ingeniería Catalíticas (GICIC)
Instituto de Investigaciones en Catálisis y Petroquímica (INCAPE)-CONICET-UNL
Ruta Nac. 168 KM 0, Paraje El Pozo, Santa Fe (3000), Argentina.
E-mail: nbertero@fiq.unl.edu.ar

Supporting information for this article is given via a link at the end of the document.

Abstract: SiO₂-Al₂O₃-supported Ru, Ir and Pt-based catalysts with moderate metal loading (1%) were tested for the first time in the production of pentyl valerate (PV) in liquid phase from γ -valerolactone, pentanol (in excess) and H₂. The acidity of these bifunctional catalysts, plays a key role in the one-pot process comprising two consecutive acid-catalyzed reactions and a metal-catalyzed one. Metal dispersion also shown to be relevant for the conversion of the pentyl pentenoate intermediate into PV by hydrogenation over the metal sites. Pt/SA catalyst with the highest surface acidity and metal dispersion reached total GVL conversion with a PV yield of 90.0% after 10 h, exhibiting a PV productivity of 300 mmol/g_M.h, i.e. a value between three and four times higher than the best result reported until now. These findings highlight the potential that noble metal-based catalyst with moderate metal loading have in the valorization of biomass-derived platform molecules such as γ -valerolactone.

A significant fraction of the worldwide energy demand comes from the transportation sector. In 2018, 28% of the whole energy produced in U.S. was used for transportation purposes ^[1]. However, 92% of this energy was supplied by fossil fuels and this is causing a serious global warming. Lignocellulosic biomass has been targeted as a promising raw material for the production of biofuels because: 1) is a kind of non-food-derived biomass; 2) is an abundant and inexpensive form of biomass; 3) it offers the energy of 30-160 billion barrels of oil equivalent (bboe) per year worldwide ^[2]. The well-known strategy for the production of biofuels from biomass comprises: (a) deconstruction of lignocellulose into platform molecules such as levulinic acid (LA) and γ -valerolactone (GVL); (b) transformation of these platform chemicals into biofuels ^[3].

Valeric esters have been regarded as attractive biofuels due to their considerably energy density, good volatility-ignition properties and appropriate polarity in comparison with current biofuels such as ethanol. Even more, depending on the alkyl group (ethyl or pentyl), these esters are perfectly compatible for gasoline or diesel pools, respectively, passing satisfactorily a 250,000 km road trial in 2010 ^[4]. Particularly, pentyl valerate (PV) has a higher volatility and better cold-flow properties and lubricity than fatty acid methyl esters (FAME), i.e. biodiesel. Besides, engine efficiency and emissions are not significantly affected when diesel is blended with PV up to 20% ^[5]. In a pioneering work, Lange et al. reported 20-50% selectivity to PV from GVL at 548-573 K and 10 bar of H₂ over Pt or Pd/TiO₂ catalysts through the hydrogenation/hydrogenolysis of GVL to pentanoic acid (PA) and subsequent esterification of PA with pentanol (PL) (ROUTE 1 of Figure 1) ^[4]. In this route, the ring-opening of GVL forms initially pentanoic acid, a very reactive key intermediate that, in the presence of metal sites and H₂, is rapidly hydrogenated over the

catalyst surface into pentanoic acid ^[4]. Then, along ROUTE 1, Yan et al. reported PV production in combination with pentanol and pentane (regarded as a biofuel mixture) from GVL without using pentanol as reagent over Pd(5%)/HY ^[6]. Although this work showed certain novelty, severe reaction conditions and a very high Pd-content were used to reach 60% yield of PV after 30 h.

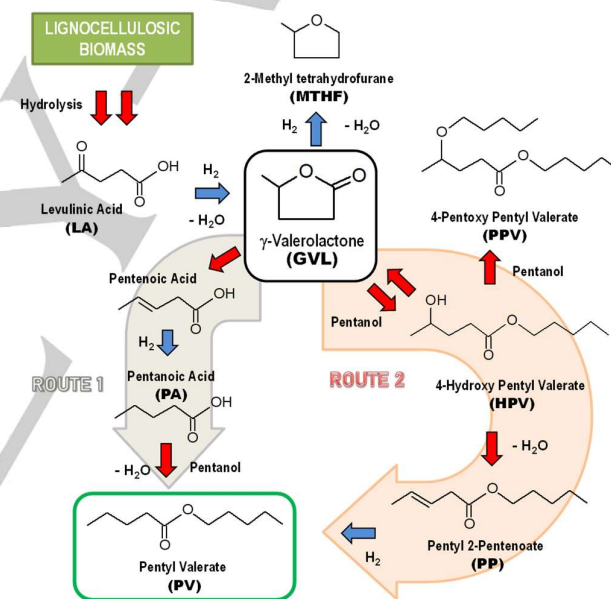


Figure 1. Reaction network, showing the two possible routes, for the one-pot production of pentyl valerate (PV) from biomass-derived γ -valerolactone (GVL) over bifunctional metal/acid catalysts [\rightarrow acid sites; \rightarrow metal sites].

On the other hand, a novel route for PV production was proposed by Chan-Thaw et al. involving the reaction of GVL, PL and H₂ over Cu-based catalysts ^[7]. In this alternative reaction path (ROUTE 2 of Figure 1), the one-pot process begins with the acid-catalyzed nucleophilic addition of PL to the carboxylic group of GVL and ring-opening giving 4-hydroxy pentyl valerate (HPV). Then, the acid-catalyzed dehydration of HPV leads to pentyl 2-pentenoate (PP), which can be hydrogenated over metallic sites to PV ^[7]. However, depending on the catalyst and reaction conditions, HPV can also react with other PL molecule to form 4-pentoxypentyl valerate (PPV) and GVL can be converted initially into 2-methyl tetrahydrofuran (MTHF) by hydrogenation/hydrogenolysis.

To the best of our knowledge, the production of PV through ROUTE 2 has only been studied over Cu ^[7-10] and Ni-based

COMMUNICATION

catalysts^[11], whereas bifunctional catalysts based on noble metal have not been tested yet. The aim of this work was to explore the potential of SiO₂-Al₂O₃-supported Ru, Ir and Pt-based catalysts with moderate metal loadings ($\approx 1\%$) to carry out this one-pot catalytic process along ROUTE 2. The main motivation of this work relies on the necessity of boosting the PV productivity in these batch one-pot processes, improving the process integration, before moving to continuous processes for a large-scale PV production^[12].

Specific details regarding preparation, characterization and catalytic tests are given in Supporting Information SI.1-3. The characterization results of the bifunctional samples are presented in Table 1. The metal loading, determined by XRF, was between 0.94% and 1%. Regarding the chlorine content of M/SA samples, important differences were detected by XRF, following the pattern: Ru/SA >> Ir/SA > Pt/SA. The pattern for the specific surface area (S_g) of the samples and the support was: SA > Pt/SA > Ir/SA > Ru/SA, whereas the pattern for the pore volume was: SA > Pt/SA \approx Ir/SA > Ru/SA, indicating a partial blockage of the pore structure of SA after impregnation with the metal precursors. The X-Ray diffractograms of calcined samples are shown in Figure 2.a. For calcined Ru/SA, Ir/SA and Pt/SA samples, only the diffraction signals of RuO₂ (PDF-731469), IrO₂ (PDF- 431019) and PtO₂ (PDF-431045), respectively were observed (more details in section SI.4) with crystalline domains smaller than 4 nm, in agreement with other authors^[13-15].

Table 1. Characterization results.

Solid	Metal load ^[a] (wt%)	Cl content ^[a] (wt%)	S_g ^[b] (m ² /g)	V_P ^[c] (cm ³ /g)	d_M ^[d] (nm)	n_A TPD ^[e] ($\mu\text{mol}/\text{m}^2$)	$L/(L+B)$ ^[f]
SA	-	-	460	0.74	-	0.59	0.78
Ru/SA	0.98	0.737	409	0.57	7.4	0.52	0.65
Ir/SA	1.00	0.059	413	0.62	6.7	0.65	0.71
Pt/SA	0.94	0.002	425	0.63	2.8	0.86	0.73

Values determined by: [a] EDXRF; [b-c] N₂ physisorption; [d] TEM; [e] TPD of NH₃; [f] FTIR of adsorbed pyridine.

The TPR profiles of the calcined samples are presented in Figure 2.b. For Ru/SA a sharp reduction peak appeared between 403-513 K with the maximum at 463 K attributed to RuO₂, detected by XRD^[13]. In the case of Ir/SA, the consumption of H₂ took place mainly between 423-583 K with a maximum at 503 K, and between 623-733 K with a maximum at 683 K, suggesting a higher heterogeneity of the IrO₂ oxide than in the case of Ru/SA^[14]. Finally, in Pt/SA a single and broad reduction peak appeared between 433-633 K showing its maximum at about 513 K related to reduction of PtO_x species showing different interactions with the SA support, in agreement with other authors over Pt/SA catalysts, prepared from PtClO₆ and with a similar Pt loading^[15]. The metal dispersion (D_M) of Ir/SA and Pt/SA samples was estimated by CO chemisorption at room temperature. D_M values were calculated assuming a stoichiometry (CO):M⁰_{SUP}=1^[13]. D_M values of about 12.6 and 27.4% were obtained for Ir/SA and Pt/SA, respectively. Assuming a cubic metal particle model, the average metal particle size for Ir/SA and Pt/SA was 8.4 nm and 4.1 nm, respectively. However, for Ru-based catalysts CO chemisorption is not a suitable technique for determining metal dispersion at the light of the possible linear and bridged CO adsorption^[16]. Besides, it has been well documented that residual chloride coming from RuCl₃ precursor blocks the CO and H₂ adsorption, leading to an underestimated metal dispersion using chemisorption techniques^[17].

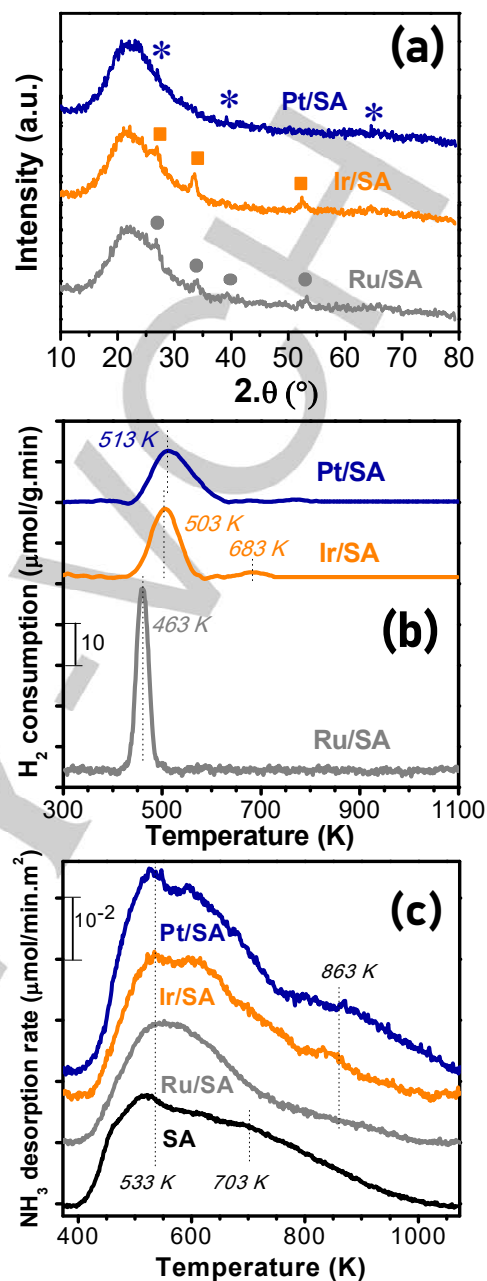


Figure 2. Catalyst characterization: (a) XRD pattern of calcined samples (● RuO₂; ■ IrO₂; ★ PtO₂); (b) TPR profiles of calcined samples; (c) TPD of NH₃ profiles from activated samples and SA; (d) TEM images of activated samples.

COMMUNICATION

Additionally, TEM results (Figure 2.d) showed the presence of metal nanoparticles for the three supported catalysts, in the ranges 1-13, 2-14 and 1-5 nm for Ru/SA, Ir/SA and Pt/SA, respectively (Fig. SI.4 of Supporting Information). The pattern for the average size of metal particles was: Ru/SA (7.4 nm) \cong Ir/SA (6.7 nm) > Pt/SA (2.8 nm) (Table 1).

Acid site density and relative acid strength of reduced samples and SA support were probed by TPD of NH₃. Results are shown in Figure 2.c and are summarized in Table 1. The evolved NH₃ from SA support was evidenced by a broad band between 393 K and 1073 K, with its maximum at 520 K and a shoulder at 703 K, indicating the presence of surface sites of different acid strength. For the three bifunctional catalysts, a broad distribution of acid strength was also observed, comprising a main band with its maximum at about 533 K and a shoulder at about 863 K. The surface acid site density (n_A) followed the pattern: Pt/SA > Ir/SA > SA > Ru/SA (Table 1). This is in agreement with the findings of other authors, reporting a higher n_A value over Ir/SA and Pt/SA compared to the SA support when the chlorine content is relatively low [14,18]. In contrast, over Ru/SA the considerable chlorine content could block not only metal sites, but also support acid sites, modifying the L/(L+B) ratio and also the strength of the minority Brønsted acid sites [17,19]. The nature of surface acid sites over the samples was determined by FTIR of chemisorbed pyridine [11] and the spectra are presented in Fig. SI.5 of Supplementary Information. The pattern for the L/(L+B) ratio (Table 1) followed: SA > Pt/SA \cong Ir/SA > Ru/SA, showing the Ru/SA sample a value 17% lower than SA support, indicating that the higher the chlorine content, the lower the L/(L+B) ratio.

The M/SA samples and the SA support were tested in the one-pot conversion of GVL into PV, performing previously a "blank" experiment (section SI.5). When GVL was contacted with PL for 8 h in the presence of SA, at 10 bar of H₂ and 523 K, a GVL conversion of 55.5%, with a PP and PPV yield of 20.5% and 12.2%, respectively (Fig. SI.7.a). However, after 8 h the carbon balance only reached 77.0%, suggesting the presence of a relatively high concentration of intermediates adsorbed on SA support [11]. The catalytic results of the one-pot production of PV from GVL, PL and H₂ through ROUTE 2 over the three bifunctional catalysts are shown in Figure SI.7 of Supporting Information and summarized in Figure 3. Due to the fact that the first two reactions of the one-pot scheme are acid-catalyzed reactions, the TOF values (Figure 3) were estimated with n_A values (Table 1) and the pattern was Ru/SA (159.6 h⁻¹) > Ir/SA (130.6 h⁻¹) \cong Pt/SA (124.1 h⁻¹). Ru/SA showed a relatively high initial GVL conversion, reaching X_{GVL} =60.6% after 8 h. The yield of the intermediate HPV was lower than 5%, whereas the PP intermediate showed an increasing yield that reached a value of η_{PP} =10.2% (Figure SI.7.b). The conversion of HPV into PP and consecutive PV (η_{PV} =16.0%) was slightly faster than the undesirable conversion of HPV into PPV (η_{PPV} =11.2%). However, after 8 h the final PV selectivity was only 26.4% and the C balance reached 78.4%, suggesting that GVL and/or intermediates remain adsorbed on the catalyst surface. In the case of Ir/SA catalyst, the GVL conversion after 8 h was 57.7%, i.e. a value slightly lower than with Ru/SA. The η_{HPV} was also lower than 5% during the run due to fast conversion into PP. However, the rate of PP conversion into PV over Ir/SA was lower than over Ru/SA, observing a η_{PP} =24.9% after 8 h (Figure SI.7.c). The HPV conversion into PPV was slightly faster than over Ru/SA (η_{PPV} =14.3%). This fact, combined with a lower hydrogenation activity of PP into PV (η_{PV} =11.9%), led to a discrete final PV selectivity of 20.6%. However, over Ir/SA the C balance reached 95.0%, a value considerably higher than over Ru/SA. Finally, Pt/SA showed an initial GVL conversion rate similar to that of Ru, but reaching a final conversion of 69.4% after 8 h, i.e. the highest value of the series of catalysts tested. The rate of

conversion of HPV to PP was higher than over Ru/SA and Ir/SA, showing η_{HPV} <3.1% and η_{PP} <3.0% during the run (Figure SI.7.d). The PV rate formation was appreciably higher over Pt/SA than over Ru/SA and Ir/SA catalysts, reaching a final value of η_{PV} =51.0% after 8 h with a selectivity of 73.5%, keeping the η_{PPV} <10%. Besides, the C balance was 94.7%, suggesting that the surface concentration of adsorbed GVL/intermediates is lower than for Ru/SA.

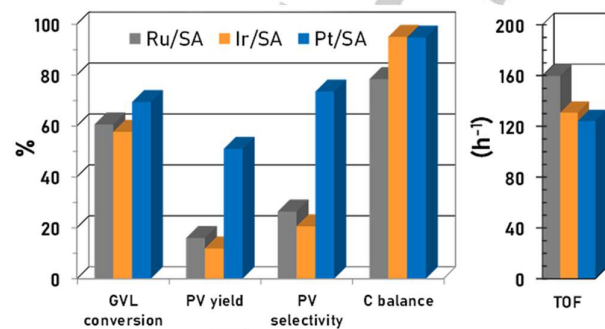


Figure 3. Catalytic performance of (■) Ru/SA; (■) Ir/SA and (■) Pt/SA [T=523 K, p=10 bar H₂, W_c=0.25 g, V_{RL}=40 mL, C^o_{GVL}=0.37 M, stirring rate=650 rpm, time=8 h].

From the characterization and catalytic tests results it is clear that the three catalysts do not have significantly different textural properties (differences of about 3.9% in S_g and 10.5% for V_p between Ru/SA and Pt/SA) and all of them are mesoporous materials as well, where a shape selectivity phenomenon cannot take place. Thus, differences in activity and selectivity to PV must be ascribed to the acid/metal site balance at the catalyst surface, where the chlorine residues can also play a role. The X_{GVL} over Ru/SA and Ir/SA after 8 h (60.6% and 57.7% shown in Figure 3) was not significantly higher than the value obtained over SA support in the absence of metal and H₂ (55.5%). This strongly suggests that the final reaction of the one-pot system, the hydrogenation of PP into PV, is not so efficiently promoted over Ru/SA and Ir/SA. Based on the values of the ratio between the initial GVL moles and the amount of acid sites $n^o_{GVL}/(n_A \cdot S_g \cdot W_c)$ =294, 233 and 171 for Ru, Ir and Pt, respectively, it is possible to infer that the catalyst surface works at a very high coverage in these samples. The final η_{PPV} at 8 h was between 10 and 14.3% for the three M/SA and SA support, indicating that the undesirable acid-catalyzed reaction HPV + PL \rightarrow PPV + H₂O is not strongly affected by the acid site density and metal dispersion. In contrast, ($\eta_{PP} + \eta_{PV}$) values at 8 h were equal to 20.5, 26.2, 36.8 and 54.0% for SA, Ru/SA, Ir/SA and Pt/SA, respectively. This is showing that the tandem involving the dehydration of HPV into PP and the subsequently PP hydrogenation into PV was promoted following the pattern: Pt/SA > Ir/SA > Ru/SA > SA. Taking into account the metal particle size and the chlorine content of bifunctional samples (Table 1), it is expected that the dissociative H₂ chemisorption would follow the pattern: Pt/SA > Ir/SA > Ru/SA. A possible and reasonable explanation of the appreciably better catalytic performance of Pt/SA can be found considering not only that each acid site must convert a significantly lower amount of GVL molecules on Pt/SA than on Ru/SA and Ir/SA, but also the fact that Pt/SA catalyst has smaller metal particles that promotes more efficiently the H₂ chemisorption and PP hydrogenation. Besides, the chlorine residues, as shown by FTIR in Fig. SI.6, modify the density and nature of surface acid sites (Table 1), leading to a lower C balance and a higher TOF over Ru/SA than over Ir/SA and Pt/SA (Figure 3), suggesting a stronger GVL adsorption that diminishes PV productivity. Particularly, this new kind of acid sites are created by the action of residual chlorine on the -OH groups of SA, as FTIR results showed. Furthermore, a modification of the H₂ chemisorption capacity of the metal

COMMUNICATION

particles by electronic effects due to this new acid sites and the residual chlorine cannot be discarded, deserving a future investigation^[19].

In summary, Pt/SA with the highest acidity and metal dispersion of the series was the best catalyst for the PV production from GVL, PL and H₂. Additional experiments varying temperature, H₂ pressure, initial concentration of GVL and catalyst/GVL ratio were carried out over this sample in order to improve GVL conversion and PV yield. Figure 4 shows the best catalytic performance obtained over Pt/SA after 10 h and using 0.5 g of catalyst, keeping constant the rest of the reported experimental conditions. In this catalytic run, a final GVL conversion of 100% and a PV yield and selectivity of 90.0% after 10 h were obtained (Figure 4).

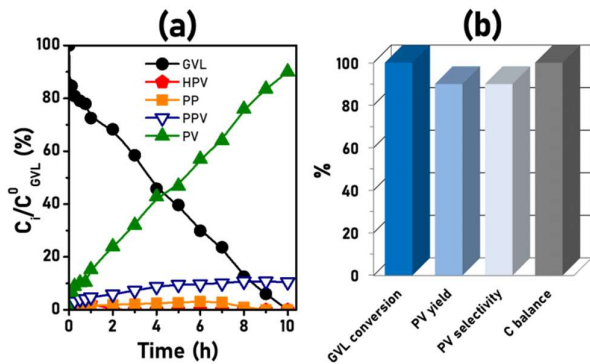


Figure 4. (a) Evolution with time of the reactant and product concentration over Pt/SA; (b) Catalytic performance of Pt/SA [T=523 K, p=10 bar H₂, W_c=0.5 g, V_{PL}=40 mL, C⁰_{GVL}=0.37 M, stirring rate= 650 rpm, time= 10 h].

Table 2 compares the previously reported catalytic performance, PV productivity and operative conditions in batch processes with our results. Although a PV selectivity higher than 90% has already been reported by other authors, in this work the PV productivity during the batch process over Pt/SA reached the highest value.

Table 2. Comparison of catalytic performance in batch processes for the PV production in liquid phase reported by other authors with this work.

Catalyst	T ^[a] (K)	p _{H₂} ^[b] (bar)	t ^[c] (h)	X _{GVL} ^[d] (%)	S _{PV} ^[e] (%)	P _{PV} ^[f] (mmol/g _M .h)	Ref.
Pd(5%)/HY	533	80	30	99	60	88.8	[6]
Cu(8%)/SiO ₂ -ZrO ₂	523	10	20	90	83	47.7	[7]
Cu(16%)/SiO ₂	523	10	10	91	92	52.3	[8]
Cu(10%)/ZrO ₂ -ZnAl ₂ O ₄	523	10	10	91.0	99.0	91.8	[9]
Cu(10%)/ZrO ₂	503	15	10	85.4	98.1	87.5	[10]
Pt(1%)/SiO ₂ -Al ₂ O ₃	523	10	10	100	90.0	300.1	This work

[a] Reaction temperature; [b] H₂ pressure; [c] reaction time; [d] GVL conversion; [e] PV selectivity; [f] PV productivity per gram of metal.

As Table 2 shows, the works employing Cu-based catalyst involving the ROUTE 2 (Figure 1)^[7-10] have shown as advantages an appreciable activity and remarkable selectivity with a relatively cheap metal but with a catalyst preparation not so simple, except the work of Liu et al.^[9]. On the other hand, in the work of Yan et al.^[6], involving the ROUTE 1, a Pd-based catalyst with high metal loading (5%) was employed and more severe reaction conditions. In contrast, in our case, with low-moderate (1%) noble metal loading a PV productivity of about 300 mmol/g_M.h was reached

after 10 h, a value between three and four times higher than previously reported values (Table 2). The highest value of PV productivity reported until now obtained in this work shows clearly the potential that Pt/SA catalysts with low-moderate Pt loadings have in the transformation of biomass-derived GVL into valuable biofuels. Not only the acid/metal balance, but also the Lewis/Brønsted nature of acid sites play a key role for boosting the PV productivity. Future approaches focused on the precise tuning of n_A (but with mainly Lewis nature) and D_M values appear to be a suitable road to success for designing continuous processes for a larger biofuel production.

Acknowledgements

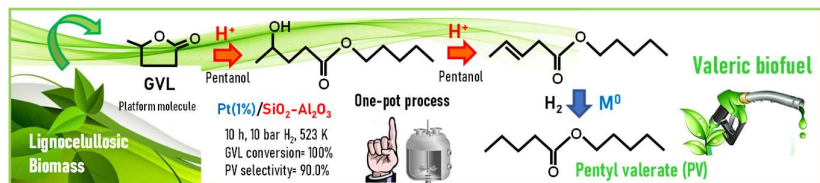
The authors thank CONICET (Grant PIP 767-2015) and ANPCyT (Grant PICT-2015-3545) from Argentina for financial support.

Keywords: batch processes • bifunctional catalysts • heterogeneous catalysis • noble metals • valeric biofuels

- [1] B.A. Babb, M.K. Pruett, *U.S. Energy Information Administration, Monthly Energy Review* **2019**, April.
- [2] G.W. Huber, B.E. Dale, *Sci. Am.* **2009**, 301, 52-59.
- [3] (a) S.N. Derle, P.A. Parikh, *Biomass Convers. Biorefinery* **2014**, 4, 293-299; (b) Z. Yi, D. Hu, H. Xu, Z. Wu, M. Zhang, K. Yan, *Fuel* **2020**, 59, 116208; (c) Z. Yu, X. Lu, J. Xiong, N. Ji, *ChemSusChem* **2019**, 10.1002/cssc.201901522.
- [4] J.P. Lange, R. Price, P.M. Ayoub, J. Louis, L. Petrus, L. Clarke, H. Gosselink, *Angew. Chemie - Int. Ed.* **2010**, 49, 4479-4483.
- [5] F. Contino, P. Dagaut, G. Dayma, F. Halter, F. Foucher, C. Mounaim-Rousselle, *J. Energy Eng.* **2014**, 140, 1-7.
- [6] K. Yan, T. Lafleur, X. Wu, J. Chai, G. Wu, X. Xie, *Chem. Commun.* **2015**, 51, 6984-6987.
- [7] C.E. Chan-Thaw, M. Marelli, R. Psaro, N. Ravasio, F. Zaccheria, *RSC Adv.* **2013**, 3, 1302-1306.
- [8] N. Scotti, M. Dangate, A. Gervasini, C. Evangelisti, N. Ravasio, F. Zaccheria, *ACS Catal.* **2014**, 4, 2818-2826.
- [9] W. Li, Y. Li, G. Fan, L. Yang, F. Li, *ACS Sustain. Chem. Eng.* **2017**, 5, 2282-2291.
- [10] S. Liu, G. Fan, L. Yang, F. Li, *Appl. Catal. A: Gen.* **2017**, 543, 180-188.
- [11] K.G. Martinez Figueredo, D.J. Segobia, N.M. Bertero, *Catal. Commun.*, **2020**, 144, 106087.
- [12] K. Yan, Y. Yang, J. Chai, Y. Lu, *Appl. Catal. B: Environm.* **2015**, 179, 292-304.
- [13] L. Chen, Y. Li, X. Zhang, Q. Zhang, T. Wang, L. Ma, *Appl. Catal. A Gen.* **2014**, 478, 117-128.
- [14] S.A. D'Ippolito, A.D. Ballarini, C.L. Pieck, *Energy and Fuels* **2017**, 31, 5461-5471.
- [15] (a) L.S. Carvalho, C.L. Pieck, M.C. Rangel, N.S. Figoli, C.R. Vera, J.M. Parera, *Appl. Catal. A Gen.* **2004**, 269, 105-116; (b) M. Vicerich, V. Benitez, M. Sánchez, C. Especel, F. Epron, C. Pieck, *Can. J. Chem. Eng.* **2019**, 98, 749-756.
- [16] (a) M. Kobayashi, T. Shirasaki, *J. Catal.* **1973**, 28, 289-295; (b) C. Gutierrez, J.A. Caram, *J. Electroanal. Chem.* **1991**, 305, 289-299; (c) G. Corro, R. Gomez, *React. Kinet. Catal. Lett.* **1979**, 12, 145-150.
- [17] (a) B. Lin, R. Wang, J. Lin, J. Ni, K. Wei, *Catal. Lett.* **2011**, 141, 1557-1568 (b) T. Narita, H. Miura, K. Sugiyama, T. Matsuda, R.D. Gonzalez, *J. Catal.* **1987**, 103, 492-495; (b) T. Narita, H. Miura, M. Ohira, H. Hondou, K. Sugiyama, T. Matsuda, R.D. Gonzalez, *Appl. Catal.* **1987**, 32, 185-190; (c) P.G.J. Koopman, A.P.G. Kieboom, H. van Bekkum, *J. Catal.* **1981**, 69, 172-179.
- [18] A. Giroir-Fendler, P. Denton, A. Boreave, H. Pralraud, M. Primet, *Top. Catal.* **2001**, 16/17, 1-4.
- [19] (a) J.B. Peri, *J. Phys. Chem.* **1966**, 70, 3168-3179; (b) N.B. Muddada, U. Olsbye, T. Fuglerud, S. Vidotto, A. Marsella, S. Bordiga, D. Gianolio, G. Leofanti, C. Lamberti, *J. Cat.* **2011**, 284, 236-246.

COMMUNICATION

Entry for the Table of Contents



Bifunctional noble metal-based catalysts of Ru, Ir and $\text{Pt}/\text{SiO}_2\text{-Al}_2\text{O}_3$, with moderate metal content, were tested for the first time in the one-pot production of pentyl valerate (PV) from γ -valerolactone (GVL), pentanol and H_2 . $\text{Pt}(1\%)/\text{SiO}_2\text{-Al}_2\text{O}_3$ converted 100% of GVL with a PV selectivity of 90% after only 10 h at 523 K and 10 bar of H_2 , leading to the highest PV productivity reported until now in a batch process.

WILEY-VCH

Accepted Manuscript